BINDING OF MYOSIN SUBFRAGMENT 1 TO GLYCERINATED INSECT FLIGHT MUSCLE IN THE RIGOR STATE

R. S. GOODY,* M. C. REEDY,‡ W. HOFMANN,* K. C. HOLMES,* AND M. K. REEDY‡

*Abteilung Biophysik, Max-Planck-Institut für Medizinische Forschung, 6900 Heidelberg, Federal Republic of Germany; and ‡Department of Anatomy, Duke University Medical Center, Durham, North Carolina 27710

ABSTRACT   The binding of rabbit muscle myosin subfragment 1 (S1) to glycerinated insect flight muscle fibers has been studied by low-angle x-ray diffraction, quantitative sodium dodecyl sulfate gel electrophoresis, quantitative interference microscopy, and electron microscopy. Changes induced in the rigor x-ray diffraction pattern are consistent with the idea that vacant myosin-binding sites on thin filaments are filled by exogenous S1. Electron microscopy indicates that S1 permeates and labels fibers and fibrils completely. Electron micrographs also show that cross-bridges are not displaced by exogenous S1 under the conditions used, and this is supported by the unchanged mechanical stiffness of the S1-labeled fibers. The amount of bound S1, as measured by gel electrophoresis and interference microscopy, together with the magnitude of the intensity changes in the x-ray diffraction pattern, is consistent with a thick filament structure that contains four molecules of endogenous myosin per 14.5 nm of its length, but does not agree well with earlier estimates of six myosins per crown. Lack of information on possible inhibition of S1-binding by factors other than the presence of cross-bridges, e.g., troponin, render uncertain calculations of the number of attached cross-bridges in the rigor state. However, it appears that at least 75% of the endogenous myosin heads are attached. Occupancy of binding sites on thin filaments after incubation with S1 is high, probably >85%, so that x-ray scattering from those parts of the structure that adhere to the symmetry of the thin filaments can be treated as diffraction from S1-decorated thin filaments. In addition, we show in thin flared x cross sections that exo-S1 heads bind to actin with the geometry described in decorated actin by Taylor, K. A., and L. A. Amos (1981, *J. Mol. Biol.*, 147:297–324).

INTRODUCTION

Insect flight muscle has an excess of actin monomers over myosin heads. Since myosin subfragment 1 (S1) is known to bind to actin with a stoichiometry of 1:1 with respect to the monomers, muscle fibers in the rigor state are expected to contain free myosin-binding sites. The number of such vacant sites in rigor depends on several parameters that are not well established at present. First, the amount of myosin present in a unit cell of the structure is not known with the same degree of certainty as the amount of actin. Evidence has been presented for six myosin molecules at each 14.5 nm repeat of the thick filament (Chaplain and Tregear, 1966; Bullard and Reedy, 1973; Reedy et al., 1973; Tregear and Squire, 1973), but also for four (Wray, 1979a; Reedy et al., 1981). Second, it is not clear what proportion of the available myosin heads form cross-bridges in rigor muscle. Third, potential myosin-binding sites on thin filaments that are not involved in cross-bridge formation could also be unavailable due to other, unknown factors. We report here the results of several approaches aimed towards quantifying free actin sites by measuring the amount of S1 that can bind to fibers in the rigor state, and discuss the effect of filling these sites on the low-angle x-ray diffraction pattern and the appearance of thin sections of S1-labeled fibers in the electron microscope.

MATERIALS AND METHODS

Proteins

S1 was prepared by digestion of myosin at low ionic strength using papain (Lowey et al., 1968) or chymotrypsin (Weeds and Taylor, 1975) and was purified as described in these publications. The molecular weight was taken as 1.15×10^5. Although other ranges were explored, rigor muscle preparations were usually incubated in S1 concentrations of 100–200 μM (bundles of 30–80 fibers; x-ray work); 45–60 μM (bundles of 1–5 fibers; force and mass measurements); 20 μM (suspended fibrils; interference microscopy and PAGE). Since the binding constant between S1 and actin is ~10^8 M^{-1} under the conditions used (Konrad and Goody, 1982), these concentrations were high enough to ensure saturation of all easily accessible binding sites on thin filaments.

Solutions

Rigor buffer contained: imidazole·HCl or MOPS·KOH (20 mM), MgCl$_2$ (5 mM), EGTA (5 mM), and NaN$_3$ (5 mM), adjusted to pH 6.8 at 4°C. S1 was diluted into or dialyzed against this buffer to give a final concentration of 2–20 mg/ml (~17–170 μM). Sodium pyrophosphate (5 mM) was included with KCl (150 mM) in this buffer to give S1-releasing

solution. This solution must be freshly made, because Mg pyrophosphate precipitates on standing. Relaxing buffer contained ATP (5 or 15 mM), and was otherwise identical to rigor buffer.

Muscle Fibers and Myofibrils

Flight muscles from *Lethocerus cordofanus* or *Lethocerus indicus* were glycerinated in a buffer of similar composition to the normal rigor buffer, except for the inclusion of 50% analytical grade glycerol (Serva, Federal Republic of Germany). The excised muscles were exposed to this solution for 2–3 d at 4°C either in vacuo or by tumbling slowly before storage at −20°C. Myofibrils were prepared from glycerinated insect flight muscle as described by Reedy et al. (1981).

Mechanical Measurements

Length-tension measurements of bundles of 1–5 glycerinated fibers exposed to S1 were performed on an apparatus constructed by R. Bremel (Department of Dairy Science, University of Wisconsin, Madison, WI) and followed procedures similar to those of White (1970). A 2–5 mm fiber segment was supported (by gluing to stainless-steel wire probes) between a silicon strain gauge (Pixie 8206, Endevco Corp., Becton, Dickinson & Corp., Mountain View, CA) at one end, and a vibrator (model 102, Ling Dynamics, Royston, United Kingdom) monitored by a displacement transducer (7DCDCT-050; Hewlett-Packard Co., Waltham, MA) at the other end. Length and tension signals were recorded on a pen recorder (Brush 200; Gould Inc., Instruments Div., Cleveland, OH). Rigor tension development (typically to 150–300 μN per fiber) was recorded with a resolution of 10–20 μN. When sinusoidal length changes of 0.2% total excursion were applied at 10 Hz, the resulting excursion in rigor tension provided a measure of stiffness (typically ranging from 50–150 μN peak-to-peak per fiber). Solutions were in 1-ml beakers, exchanged by lifting the fibers from one to immerse in the next. For these experiments, fibers were evaluated by cycling relax-to-rigor 3–6 times, stretched to a relaxed state tension of 10–20 μN per fiber, then rigorized. After reaching a steady rigor tension, fibers were transferred for 1 h to S1-rigor solution containing 45–60 μM S1 where tension and stiffness were monitored, and were finally returned to MgATP-relaxing buffer. Baseline drift (20–60 μN/h) was estimated by slackening fibers to zero tension while relaxed.

X-ray Diffraction

Most of the x-ray diffraction data reported here were obtained using the mirror-monochromator camera at the Deutsches Elektronen Synchrotron (DESY), Hamburg, Federal Republic of Germany (Barrington Leigh et al., 1976) or a similar camera (X-11) on the storage ring (DORIS). For comparisons of the absolute intensities of the S1-labeled and rigor patterns, some exposures were taken using a mirror-monochromator camera on a large diameter rotating copper anode x-ray tube (Rosenbaum, 1979) using characteristic K-alpha radiation. This arrangement produced a beam geometry and intensity that was stable for several days.

Samples were mounted in one of two types of cell. The first type is a sealed flow-through cell containing a small volume ($\sim$100 μl) of solution that could be exchanged using a peristaltic pump and an external reservoir. The second type is an open cell with a minimum volume of $\sim$500 μl. In both types, the muscle fibers were fixed to stainless-steel pins or plastic supports between Mylar windows using cellulose nitrate dissolved in acetone as glue. 30–80 fibers of minimum length (1 cm) were used. The sample could be stretched after gluing by adjusting one of the pins. Normally, a test exposure was made to check specimen orientation and camera performance before beginning an incubation with S1. The incubating solution of S1, in rigor buffer at 0–4°C, was stirred by constant pumping in the flow-through cell, or by 2–5 min of gentle squirting with Pasteur pipette repeated every 1–2 h in the open cell type. A cocktail of protease inhibitors was included in the S1 incubating bath for two experiments that were finally fixed for electron microscopy, and that both gave better electron microscopic (EM) appearances than were obtained without such inhibitors. This cocktail included phenylmethanesulfonyl fluoride PMSF (1 mM), ovalbumin trypsin inhibitor (2 mg/ml), and in one of the two experiments, iodoacetate (5 mM).

The intensities of the strongest equatorial reflections (10.0 and 20.0) were measured using a position-sensitive linear detector of the delay-line type built by A. Gabriel (European Molecular Biology Laboratory [EMBL], Grenoble, France). Pulses from the detector were stored in a Northern Scientific TN 1700 multichannel analyzer (Tracor Northern, Middleton, WI), and background subtraction and estimation of the integrated intensity of the peaks were performed using the same instrument. Incident beam intensity was monitored just in front of the specimen using an ionization chamber (constructed by A. Harmsen, EMBL, Hamburg, Federal Republic of Germany). The intensity was integrated over the duration of an exposure so that during exposures in which the beam position was stable, the intensities of the strongest equatorial peaks could be normalized and compared. Films were densitometered using an drum scanner (Optronics Laboratories, Inc., Orlando, FL) on-line to a Nord-100/500 computer (Nord Computers, Oslo, Norway) as described previously (Holmes et al., 1980).

Electron Microscopy

Samples for electron microscopy were routinely prepared using x-ray monitoring, as described in Reedy et al. (1983). Fiber bundles were not fixed until binding of S1 appeared to be complete, as judged by x-ray diffraction. A modified fixation method was used (Reedy and Reedy, 1984) that was found superior to standard procedures (Reedy, M. K., manuscript in preparation). After removal of excess S1 by washing the fiber bundle for 30 s each three changes of cold rigor buffer, a fixative containing 2.5% glutaraldehyde, 2 mg/ml tannic acid, and $MgCl_2$ (10 mM) at pH 6.8 in normal rigor (MOPS) buffer was added, and the fixation was allowed to proceed for 1 h at 4°C. After three 10-min rinses in rigor buffer, secondary fixation was carried out for 15–30 min at 0°C using 1% OsO_4 in phosphate buffer (100 mM) with $MgCl_2$ (10 mM) at pH 6.0. Following water rinsing (10 min) and block staining in 1% uranyl acetate (1–12 h), the bundle was dehydrated in graded ethanol-water mixtures and embedded in Araldite 506 (CIBA-Geigy, Summit, NJ) according to Reedy et al. (1983). Most sectioning was carried out on blocks in which rigor and S1-loaded fibers had been co-embedded adjacent and parallel, so that differences in section thickness and staining would not affect the comparison of the two experimental states.

Quantitative Polyacrylamide Gel Electrophoresis

SDS-electrophoresis on cylindrical polyacrylamide gels (7.5%) was performed according to Ziegler et al. (1974) on fibrils and fibers before and after labeling with S1. For quantitative measurements, fibrils at $\sim$1 mg/ml were incubated for 5 min at 4°C with chymotryptic S1 (1–2 mg/ml) in rigor buffer containing 1 mM dithio erythritol (DTE). The fibrils were pelleted by centrifugation, washed briefly with rigor buffer, and pelleted again. After discarding the supernatant, the pellet was dissolved in hot SDS-containing sample buffer before application to the gel. Gels were stained with Fast Green as described by Potter (1974), and after destaining were scanned using a gel scanner (model CDS 200; Beckman Instruments, Inc., Fullerton, CA). Calibration staining curves were obtained for heavy chain bands of myosin and S1 from rabbit muscle in terms of original intact protein molar concentrations determined by the Lowry method and using molecular weight ratios of (heavy chain)/(heavy chain + light chains) of 200:240 for myosin and 95:115 for S1. Staining of the S1 heavy chain showed a 1.2 times greater optical density than an equivalent mass of myosin heavy chain, and the values for the ratio of bound exogenous S1 to endogenous myosin in labeled myofibrils were corrected accordingly. In control experiments, ATP was included in the S1/fibril incubation mixture. Here it was found that 5–10% of the amount bound under rigor conditions could still bind, and this was treated

as nonspecific binding or adsorption to either the fibers or to the centrifuge tube.

Quantitative Interference Microscopy

Dry mass changes in single *Lethocerus* fibrils produced by binding and release of S1 were measured by scanning interference microscopy, taking the integrated optical path difference (IOPD) over the fibril as a direct measure of its dry protein mass. A scanning integrating microinterferometer (M86; Vickers Instruments, Inc., Malden, MA) was used (in the Department of Pathology, University of Freiburg, Freiburg, Federal Republic of Germany, through the kindness of Drs. Kiefer and Sandritter). Since this instrument is not well known, a few of its essential features should be described here. It measures optical path difference (OPD) or IOPD electrooptically and displays the result on a digital readout in an arbitrary six digit form which can easily be calibrated in terms of protein mass (Goldstein and Hartmann-Goldstein, 1974). In our work, only serial comparisons mattered, so calibration was not needed. The linear OPD range for the microinterferometer (0.90 wavelengths) was about twice as great as the maximum retardation obtained over any *Lethocerus* fibril, so integration in scanning mode was clearly feasible. In all our experiments, the 75 × water immersion objective was used with the smallest scan raster; thus each 5-s scan, measuring successive spot OPDs at a rate of 10 kHz, swept the 0.38-μm laser beam through 50 lines in a raster measuring 26.7 μm × 26.7 μm at the specimen plane, to accumulate up to 50,000 spot values (depending on mask size) as required to generate and display one IOPD value (Goldstein and Hartmann-Goldstein, 1974).

A drop of fibril suspension was settled for 30 s on a coverslip before inverting and pressing it onto a glass slide between two long parallel silicone grease stripes. The stripes defined a 2–4 mm wide channel for rapid positive flow. A straight fibril adherent to the coverslip showing neither overstretch nor contraction bands was selected. This standard sarcomere pattern corresponds to the predominant appearance in thin sections. In these, the AO-band (filament overlap zone of the A-band) shows full overlap with exact matching of thin filament length to the full length of the cross-bridge zone on thick filaments. Such an AO-band averages 83% of sarcomere length in *Lethocerus*. There is no proper I-band; only ~40 nm of bare thin filament extends between the cross-bridge zone and the Z-band border.

The selected fibril was oriented north-south by stage rotation, and the rectangular masking aperture was adjusted to frame a segment 6 to 9 sarcomeres in length. Initially the instrument was set to stationary spot reading mode, and OPD in adjacent background was adjusted to read 0.100 wavelengths in the usual way by rotating the substage polarizer. The microinterferometer was then switched to scan mode for fibril mass measurements. Each full set of scan readings in our experiments was the mean from six consecutive scans of IOPD made with the mask over the fibril, corrected by subtraction of six background scans just lateral to the fibril. Mask positioning, focus checking, scanning, data recording, and calculating background corrections by a team of two operators required 1.5–2 min for each set of (6 + 6) IOPD values. Before adding S1, baseline fibril mass was established as the mean of three to five such sextuple reading sets. Gross and rapid changes during binding or release of S1 could be followed by serial single readings over the fibril without the moment-to-moment background readings and repetitions needed for maximum reproducibility.

Filter paper wicks were applied to one side of the coverslip to draw irrigating solutions of S1, pyrophosphate, etc., through the narrow
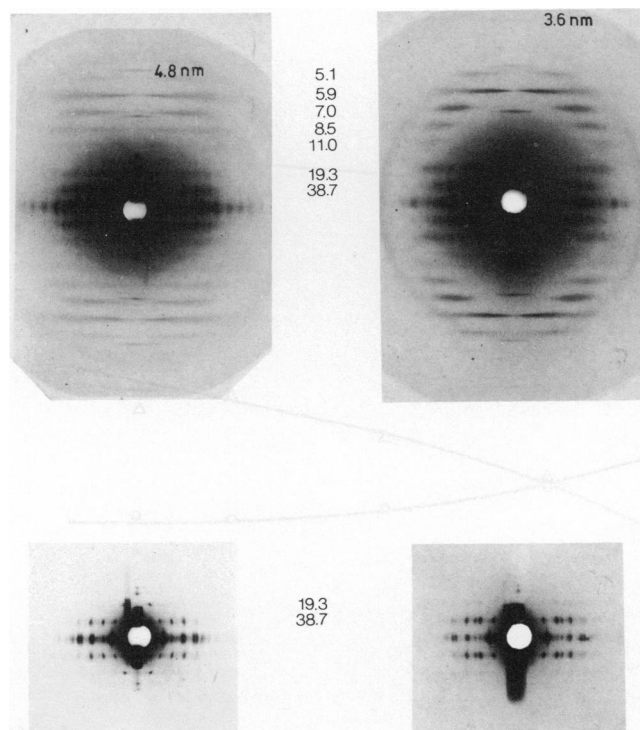

FIGURE 1   Low and medium angle x-ray diffraction patterns of glycerinated insect flight muscle in rigor (*left*) and after incubation for 24 h in papain S1 (20 mg/ml) at 4°C (*right*). The upper diagrams show the top film of a pack of six, the lower ones the third film. The layer lines can all be indexed on a 232-nm repeat, of which the 6th (38.7 nm) and 39th (5.9 nm) orders are prominent in the rigor state. After incubation in S1, the continuous layer lines are more intense and form a helix cross centered at 5.5 nm and at the origin, in contrast to the ladder pattern in rigor. X-ray source, Deutsches Elektronen Synchrotron (DESY) Hamburg, Federal Republic of Germany, running at 6 GeV and ~6 mA, exposure time 9 h for rigor, 7.2 GeV and ~10 mA, exposure time 4 h 18 min for S1-loaded fibers. Film: Ilford Industrial G. x-ray film (Ilford, Ltd., Essex, England).

channel. Visible effects of irrigant solution on fibrils usually developed 3–10 s after starting flow. The grease stripes also physically stabilized focus by minimizing coverslip flexing during irrigation. This was desirable when we wished to measure IOPD during the first moments after irrigation began, since setting the scanning mode on the microinterferometer interrupts specimen viewing and precludes real-time focus checking. The temperature was 23–25°C. To avoid progressive concentration of irrigant solutions due to evaporation during long incubations, we renewed irrigation with a fresh drop from stock solution every 5–10 min.

RESULTS AND DISCUSSION

X-ray Diffraction

The effect on the low-angle x-ray diffraction pattern of incubating glycerinated insect flight muscle fibers in S1 can be clearly seen in Fig. 1. The changes develop relatively slowly when large fiber bundles are incubated in 10–20 mg/ml S1. The time course in one particular experiment is shown in Fig. 2. The intensities of the two strongest equatorial peaks, 20.0 and 10.0, are used as signals of binding. In the particular experiment shown, the half-life for saturation with S1 was found to be ~70 min. This was determined from the time dependence of the change in ratio between the two peaks, since possible slight instability of the beam over long periods made direct measurements of the absolute intensity unreliable. Using this half-life together with measurements of the absolute

intensities of the individual reflections at shorter time intervals (i.e., before complete saturation, but while the beam position was still stable), it could be calculated that the 10.0 reflection fell ultimately to 56% and the 20.0 rose to 124%, respective, of their original values. This corresponds to a change in ratio (20.0:10.0) from 1.7 to ~4.0.

In addition to the changes on the equator, large changes occurred in other parts of the diffraction pattern (Fig. 1). The near-meridional parts of the 38.7-nm and 19.3-nm layer lines became weak compared with the rest of the pattern, and the continuous actin-based layer lines at higher angles became stronger. Comparison of absolute intensities between rigor and S1-labeled states was not easily achieved using the synchrotron source due to large fluctuations in beam intensity. This problem was not completely solved by monitoring the incident beam intensity with an ionization chamber in the beam line, since small movements of the electron path in the synchrotron caused movement of the beam relative to the sample. For this reason, a rotating anode source equipped with a mirror-monochromator camera was used to obtain a scale factor between the patterns from S1-labeled and rigor muscle. Since the camera used had a short specimen-film distance, only the outer, nonsampled layer lines were used for this comparison. It was found directly that the integrated intensities were approximately a factor of 4–5
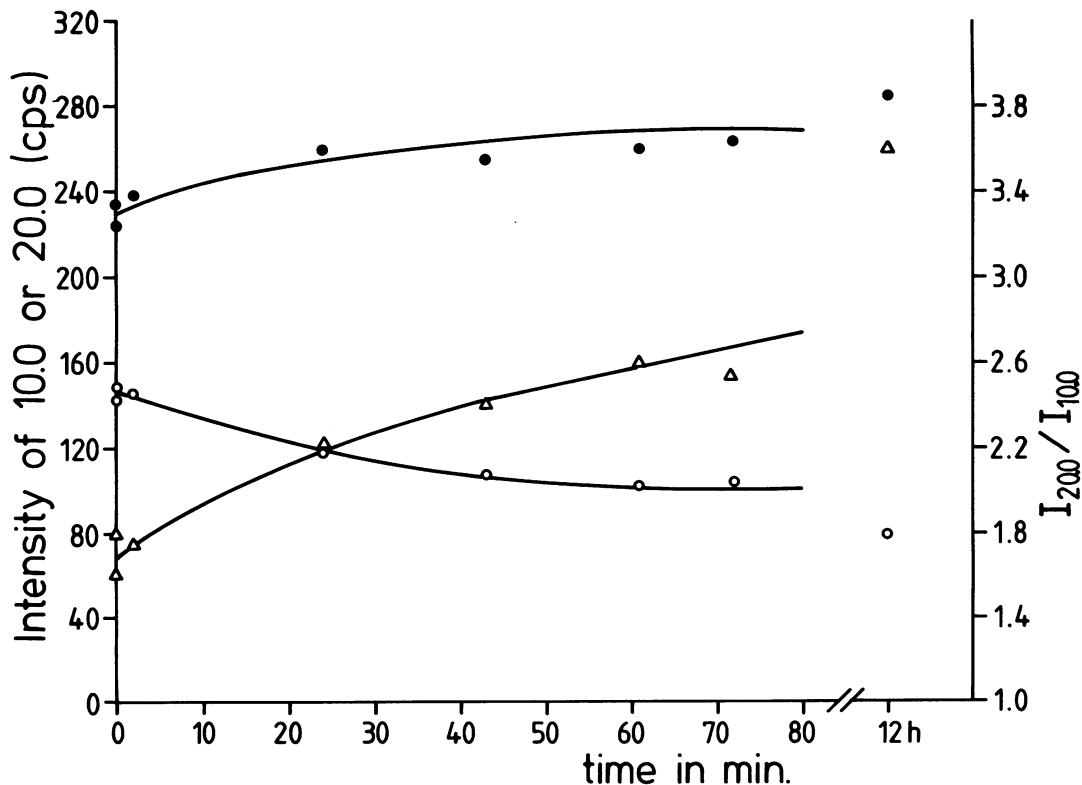

FIGURE 2   Time dependence of the changes in the intensities of the two strongest equatorial peaks (10.0, O——O, and 20.0, ●——●) and in their ratio (△——△) in the diffraction pattern from glycerinated insect flight muscle on incubation in papain S1. The intensities were measured using a linear position-sensitive detector (see Methods) on the DESY camera. The conditions were 20 mg/ml papain S1 in the standard rigor buffer (see Methods) at 4°C.

stronger after saturation with S1. In principle, film intensities can also be normalized using the detector information mentioned above on the relative strengths of the strongest equatorial peaks, and modifying all intensities by a constant factor until the 20.0 peak of the S1 pattern is 124% of that from the rigor pattern. This was not considered reliable enough to use as the only means for determining the relative strengths of the outer layer lines, because the large dynamic range of these data could easily have led to possible errors in the scaling of individual films from one data set. Fig. 3 shows intensity profiles of the nonsampled layer lines from synchrotron exposures of fibers in the rigor and in the S1-labeled states, normalized so that the integrated intensity in the 20.0 reflection from the same data set was equal in both cases. Since the actual intensity in the 20.0 peak increases $\sim \times 1.24$ on binding S1, the real difference in intensities of these layer lines is actually larger than shown here, but the above-mentioned uncertainties in scaling the six films from one exposed pack do not justify more exact normalization. As shown in Fig. 3,
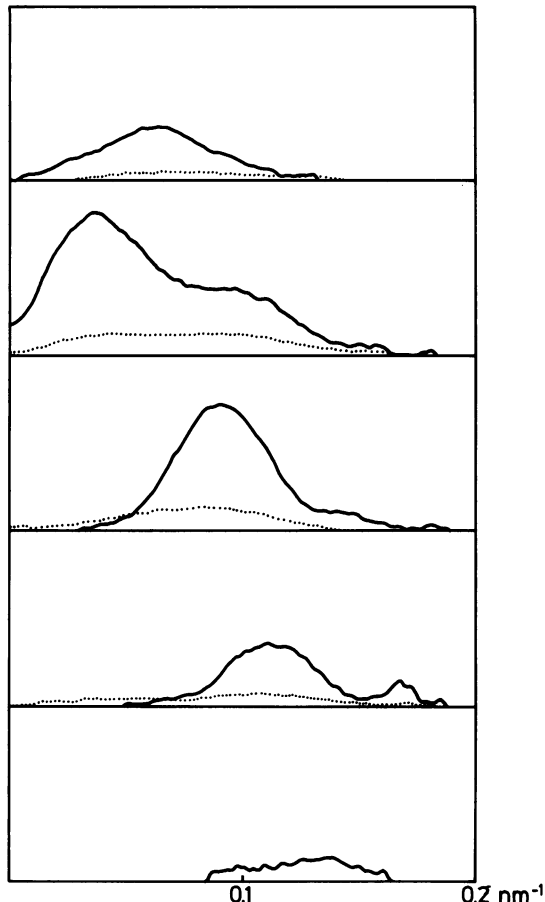

FIGURE 3 Relative intensities along the continuous actin layer lines of the diffraction patterns from insect flight muscle in the rigor state (· · ·) and fully labeled with S1 (——). The two sets of data were normalized using the factor obtained as described under Results. The traces correspond to, from *top* to *bottom*, layer lines 15, 13, 11, 9, and 7, respectively, indexed on the thin-filament repeat of 77.3 nm.

the increase in intensity, despite the inexact normalization, agrees approximately with the factor of ~4–5 obtained by direct comparison of the outer layer lines in serial film exposures obtained using the rotating anode source.

The increase in intensity of these layer lines is in harmony with the idea that the amount of density scattering with the symmetry of the actin filament is approximately doubled on saturation with S1. As discussed below, if we assume that exogenous heads scatter x-rays essentially like endogenous heads, this density doubling implies that the number of actin sites accessible to S1 in rigor is about equal to the number of sites occupied by rigor cross-bridges.

Quantitative Gel Electrophoresis

S1 binding to myofibrils or whole glycerinated fibers could be easily demonstrated by SDS gel electrophoresis. The stoichiometry of binding to myofibrils was determined by densitometry of gels stained with Fast Green. For these experiments, it was preferable to use chymotryptic S1 because of the much better homogeneity of the heavy chains compared with papain S1 as seen on SDS gels. Binding of S1 could be largely prevented by the simultaneous presence of ATP. The small amount of S1 binding that still occurred despite ATP was regarded as nonspecific, and was incuded in the background value which was substracted from each S1 measurement. However, note that this may in fact lead to an underestimate of the amount of S1 that can be bound, since the binding seen in the presence of ATP might be due to a small fraction of S1 in the preparations used, which can bind site specifically to actin even in the presence of ATP. This could be due to the presence of SH-modified S1 (possibly due to oxidation), since it is known that extensive modification of the SH groups yields S1, which cannot be readily dissociated from its complex with actin (Pemrick and Weber, 1976; this point is discussed in more detail below). Thus the value derived below for the amount of S1 bound to the fibers should be regarded as a lower limit, and the real value could be ~5–10% higher.

The number of S1 heavy chains bound reversibly to the myofibrils was quantified in relation to the number of myosin heavy chains (and thus heads) already present in the fibers (endogenous insect myosin was assumed to stain as whole rabbit myosin), and the molar ratio S1-heads/myosin-heads was calculated to be 0.92 + 0.05 from a series of measurements on myofibrils. This value was not changed significantly by changing the temperature from 4 to 23°C or by increasing the length of the incubation time from 5 to 60 min.

This result cannot be interpreted without a knowledge of the amount of myosin in the unit cell of the myofilament lattice. This has been a point of controversy in recent years, so we shall initially consider both suggestions that have been put forward, namely, that either four or six myosin molecules are present per 14.5 nm length of each thick

filament. For the purposes of this and subsequent discussion, we define here a unit of the structure that will be called a crown cell. This unit contains one crown of one thick filament (i.e., it has a length of 14.5 nm) and three thin filaments of the same length. Thus it contains either four or six myosin molecules (eight or twelve heads) and 15.75 actin monomers. The number of exogenous S1 heads that can attach to the crown cell, according to the result given above, is either 7.4 (i.e., 0.92 × 8) or 11.04 (i.e., 0.92 × 12), indicating that either 8.4 or 4.7 actin monomers remained unavailable due to prior occupation by rigor cross-bridges or other factors (see Table I).

Quantitative Interference Microscopy

When applied to fibrils at 1–20 mg/ml, S1 produced two phases of increase in fibrillar dry mass. The rapid early
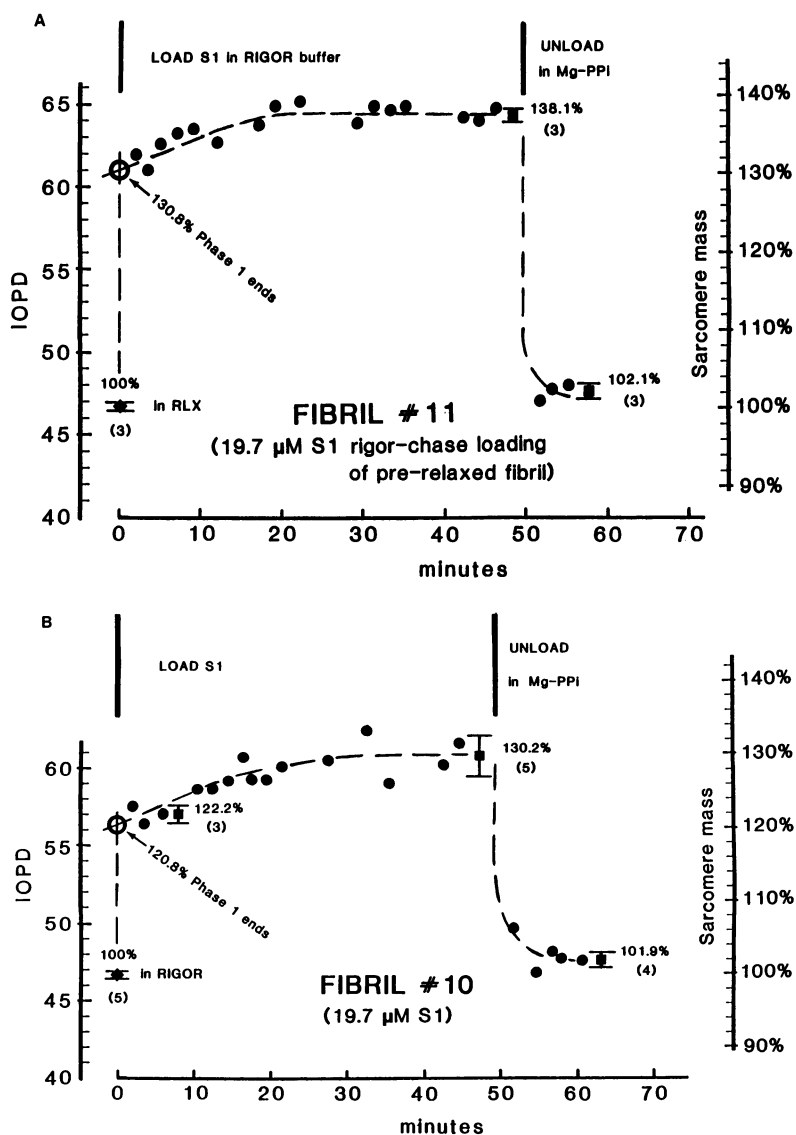

FIGURE 4 Graphs show time sequence of microinterferometer measurements of relative dry mass during two different experiments, indicating binding and release at 23–25°C of S1 to rigor (B) and to prerelaxed (A) single Lethocerus flight myofibrils in segments exactly 7 sarcomeres long. IOPD is the integrated optical path difference (between specimen and background) in arbitrary machine units (protein content is ~4.5 pg/sarcomere). Each measurement (●) is the mean of six readings, calculated from twelve IOPD scans obtained in the sequence: three over right background, six over fibril, three over left background. 100% mass level (♦) is taken as mean of (N) measurements completed just before S1 irrigation. Subsequent mean (■) and standard deviation are shown following groups of (N) just-previous measurements. Note that (a) rapid and slow phases of binding, (b) reversibility with Mg-pyrophosphate, and that (c) phase 1 binding is 1.5 times higher for prerelaxed fibril than for rigor fibril. The circled intercept of phase 2 slope at time zero is taken as peak value for phase 1 loading. Averaged results from these and other technically satisfactory measurements of phase 1 binding levels (Reedy, M.K., and R. S. Goody, manuscript in preparation) were rigor fibrils, 20.13% ± 0.51% SD (N = 12), and prerelaxed fibrils, 30.53% ± 1.14% SD (N = 6). The ideal experiment was realized in two cases, where the post-rigor loading was performed after postrelax loading (and prompt pyrophosphate unloading) had been completed on the same fibril.

phase, completed by 10–30 s, was followed by a second phase, which tended to level off after 30–60 min (Fig. 4). Although the total increase over 1 h was completely and rapidly reversible with Mg-PPi, the slow phase was considered probably nonspecific binding, possibly of aggregates, because when sufficiently prolonged, it commonly reached levels in excess of the 34% total mass increase, which would fill all existing actin sites with exoheads. The rapid initial phase, taken here as specific binding and thus as a measure of available actin sites, produced 20% mass increase in rigor fibrils, but gave a 30% mass increase in relaxed fibrils that were washed free of ATP by the same rigor solution that carried in S1 (legend, Fig. 4). These two different experiments are shown on two different fibrils in Fig. 4, but also gave such results when both were serially performed on the same fibril. This rigor + S1 chase, performed easily on a small fibril but not on whole fibers, must flush out free ATP and bring in nucleotide-free S1 in a fraction of a second at the flow velocities observed microscopically; this exo-S1, which does not have ADP and Pi at its active site, may immediately fill all of the available actin sites exposed in the relaxed state, before any relaxed endogenous heads can begin to release the bound nucleotide, which keeps them relaxed.

Assuming a molecular weight of 115 kdaltons for chymotryptic S1, it can be calculated what percentage mass increase in the whole sarcomere should be produced by binding of one S1 per crown cell. Recent studies (Reedy and Lucaveche, 1984) have confirmed that the AO-band refractive index requires a mass concentration of 0.17 g/ml, as originally established (Reedy et al., 1973), rather than the mass concentration of 0.13 g/ml expected on the basis of filament mass and lattice spacing. Although we do not know the source of this excess mass, it is clear that baseline dry mass in the insect AO-band must be taken as 0.17 g/ml for the present interferometric study. This gives a value of 4,320 kdaltons per crown cell of 58 nm side and 14.5 nm length. Each S1 of 115 kdaltons would add 2.66% to such an AO-band. If Z-band peak and H-band trough approximately cancel (as demonstrated by Reedy et al., 1973), so that average mass thickness along the whole fibril before S1 loading is originally uniform and equal to that of the AO-band, then a 2.66% increase occurring only in the AO-band, which is 83% of *Lethocerus* sarcomere length, must correspond to a 2.21% mass increase for the whole sarcomere.

Taking the 20.13% mass increase of the fibrils seen in the rapid phase described above as being due to specific binding of S1, this indicates that 9.11 S1 molecules can bind to each crown cell in the rigor state, so that 6.64 of the total number of 15.75 actin monomers are blocked by cross-bridges or other factors. The 30.53% mass increase seen on washing out relaxing solution with S1 gives a lower limit of 13.82 for the maximum number of binding sites per crown cell that are available, either to endogenous or exogenous heads. The remaining 1.9 sites could be blocked by troponin (believed to be present to the extent of 2.25 molecules per crown cell), or by unknown components, by steric hindrances to full penetration, or could represent a fraction of the endogenous heads that compete successfully with the incoming S1. (Despite the EGTA present, the progressive binding of exoheads would be expected to progressively activate the regulated thin filaments with respect to the ATP-charged endoheads). The difference between 13.82 and 9.11 gives 4.71 as the lower limit for the number of endogenous heads per crown cell attached to thin filaments as cross-bridges in the rigor state.

Electron Microscopy

Electron microscopy of thin sections and optical diffraction were done on rigor insect flight muscle that had been exposed to S1 and fixed under x-ray diffraction monitoring to obtain information about the pattern of S1 binding to whole glycerinated fibers. In particular, we were interested in determining whether penetration throughout the fiber bundle occurred in an x-ray diffraction experiment, and whether uniform labeling of the A-band occurred. Early experiments gave embedded samples that showed nonuniform labeling (i.e., some fibrils and individual sarcomeres did not differ greatly from rigor structure), swelling of sarcomeres to give a barrel-shaped appearance, and partial loss of finely ordered structure. Since previous observations had indicated that residual proteolytic activity in the S1 preparations might be responsible for these effects, multiple protease inhibitors were included in later incubations (see Methods). This step, introduced together with a tannic acid fixation procedure, dramatically improved the preservation of x-ray diffraction patterns and the quality of electron micrographs from S1-labeled fibers. The tannic acid procedure alone has improved preservation of muscle fibers fixed in other starting states, (rigor, ATP, or APPNP; Reedy, M. C., M. K. Reedy, and R. S. Goody, manuscript in preparation). It is not clear whether inclusion of protease inhibitors or the modified fixation procedure alone resulted in improvement of S1-loaded fibers. X-ray diffraction patterns of unfixed muscle in rigor and after S1-incubation can be compared with those from the finally embedded specimens in Figs. 5 and 6. For further comparison, optical diffraction patterns from micrographs of thin sections of the same x-ray monitored rigor and S1 loaded bundles are shown in Fig. 7.

In both cross and longitudinal sections virtually all fibrils and sarcomeres (>95%) from muscle incubated with S1 showed extra material uniformly labeling thin filaments by comparison with rigor, and no extraneous material could be found in or around the fibrils, e.g., clinging to the Z band or M line. The thin filaments appeared exclusively and completely labeled along their length and at all depths in every fiber and fibril.

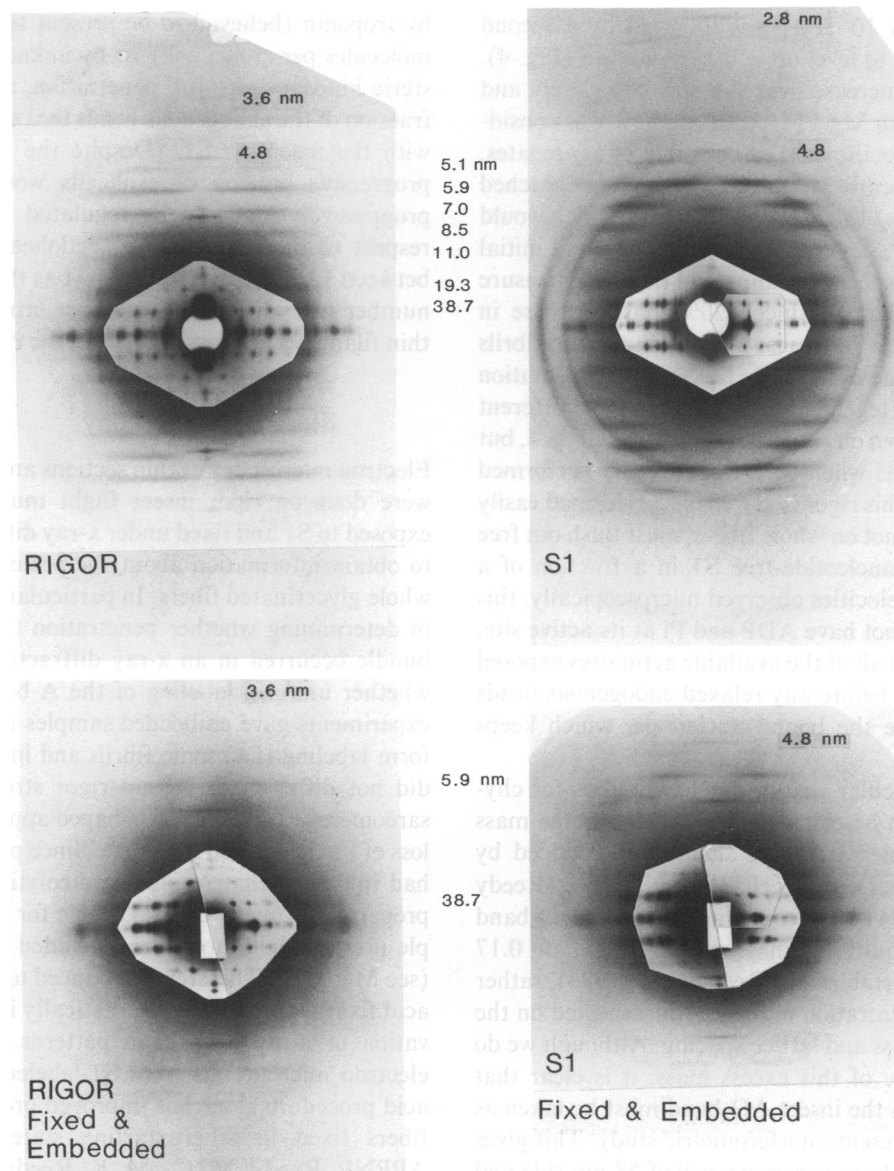Thick cross sections show increased diffuse density around the thin filaments by comparison with rigor (Fig.

FIGURE 5   Effect of fixation and embedding on the low and medium-angle x-ray diffraction patterns from rigor (*left*) and S1-loaded fibers (*right*). The fibers were incubated 39 h in chymotryptic S1 (20 mg/ml) in the presence of 1 mM PMSF and 0.5 mg/ml egg trypsin inhibitor. Taut oriented fibers loaded S1 without significant lattice swelling (in contrast to bulging of A-band sometimes seen by light or electron microscopy in fibrils, where orienting tension is presumably zero). Final lattice shrinkage after primary fixation in the presence of tannic acid varied from 15% (*inset lower left*; *inset* and *outset* from different bundles) to 1–3% (*outset lower left* and whole pattern, *lower right*). X-ray source: Storage-ring (DORIS) at DESY (Hamburg, Federal Republic of Germany) running at 3.2 GeV and 10–80 mA, exposure time 20–40 min. X-ray film Agfa Osray T4 or Kodirex for Figs. 5 and 6.

8). In thin (15 nm) cross sections (Figs. 9 and 10), the rigor flared × is seen. Although not obscured by S1 labeling, its limbs appear slightly thickened. The thin filament segment flanking the flared ×, i.e., the interdoublet gap that is normally unoccupied in rigor (Reedy and Reedy, 1985; Taylor et al., 1984), is heavily labeled with S1, showing the same sense of slew as rigor cross-bridges and decorated actin. The shape and sense of slew of flared × limbs remain as in rigor.

Single-filament myac layers (alternate thick and thin filaments) loaded with exo-S1 (Fig. 11) appear subtly

different from rigor in that the gaps between the bridges, both within and between double chevrons, appear somewhat filled in. Actin layers show more dramatic changes (Fig. 12). As described by Reedy and Reedy (1985), adjacent thin filaments receive rigor cross-bridges at different angles (alternatively +60° and −60°) to the section plane. The resulting pattern of interfilament rungs and staggered beads makes adjacent thin filaments nonsuperimposable (unless rotated end-for-end). However, when loaded with S1, adjacent thin filaments appear nearly superimposable and simply staggered. Nevertheless, adja-

cent thin filaments are still not fully superimposable in S1-loaded muscles, indicating that some differences persist, either in shape and (or) size, or staining intensity, between cross-bridges and exo-S1.

This point is also illustrated in thick cross sections (Fig. 8). In rigor such sections show that the complex of cross-bridges bound along the actin target zones on each thin filament label a restricted azimuth rather than a complete circle, thus often showing up as paired densities, bracketing a center of lower density. This core structure of density remains in the S1-labeled thick cross sections, but is completely surrounded by a less dense halo. This demonstrates that the rigor cross-bridges are still present after S1 loading, and again suggests that bound exo-S1 is not identical with cross-bridges.

The S1-decorated flared × images give a bonus: they independently confirm Taylor-Amos binding geometry of myosin heads to actin. The two-dot appearance of the nonbridged actins in rigor flared × images and filtered images (Fig. 10 A; Fig. 13 A, B) is believed to represent the two actin long-pitch helical strands, despite the somewhat excessive separation between the dots (Reedy and

Reedy, 1985; Taylor et al., 1984). When S1 decorates the actin at this position, the filtered image (Fig. 10 B) corresponds closely to the profile expected (Fig. 13 C) if bound exoheads maintain the geometry with respect to the actin dyad azimuth, which was first described from three-dimensional reconstructions of S1-decorated actin by Taylor and Amos (1981).

Tilted views of S1-labeled sections provide further evidence that bound exogenous S1 does not displace cross-bridges. If S1-myac layers are tilted around a longitudinal axis (Figs. 14 and 15), center-beading and straddle-beading patterns along actin, which are characteristic of rigor cross-bridge shapes and distibution, are intensified every 38.7 nm (Reedy and Reedy, 1985). This represents the clearest demonstration that exo- and endoheads are not identical, since if they were, such rotation should produce only an apparent axial translation of the helically labeled thin filaments, but no other change in appearance. Tilting around a transverse axis (analyzed for rigor by Reedy and Reedy, 1985) also reveals the presence and persistence of cross-bridges, projecting from helically deployed origins on thick filaments to attach to thin filaments (Fig. 16).
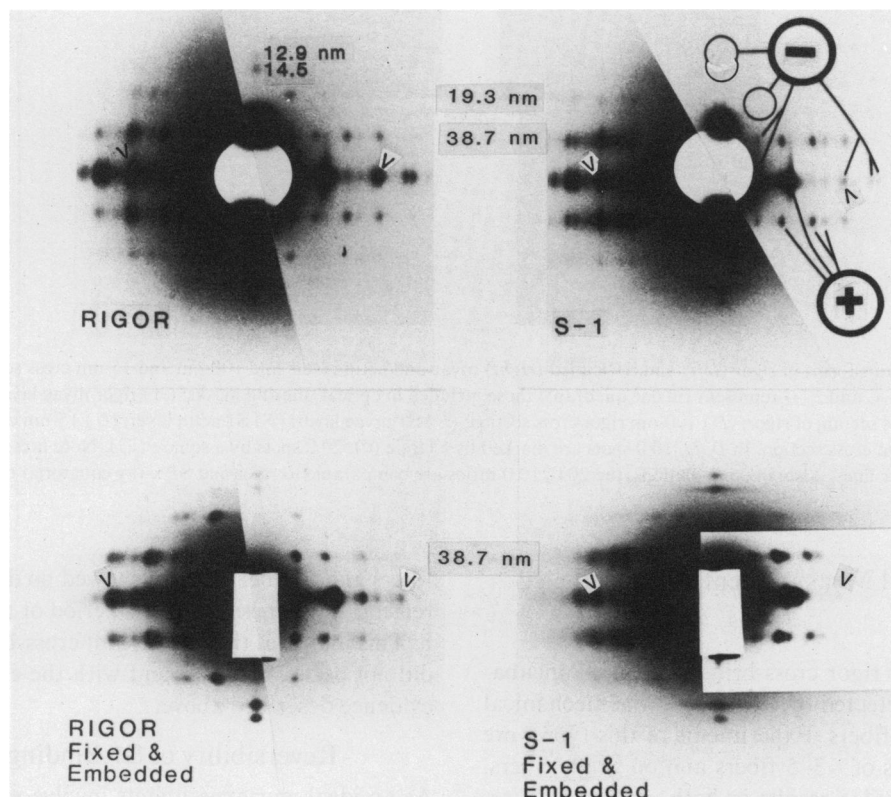

FIGURE 6   Inner sampled x-ray layer lines of unfixed and fixed rigor (*left*) and S1-loaded fibers (*right*) are shown. Arrowheads identify 31.0 reflections, demonstrating 15% lattice shrinkage by fixation-embedding for this particular rigor specimen but much less for S1. In the unfixed S1 specimen, some reflections are weakened ($\ominus$) while others are intensified ($\oplus$) compared with rigor. S1 loading causes characteristic first row-line weakening on 19.3 nm and 38.7 nm layer lines. This remains recognizable after fixation-embedding, as does the related outward shift of intensity maximum on 38.7 nm layer line from 10.6 to region of 20.6–30.6 reflections. Splitting of the stronger reflections in the embedded S1 sample indicates dual lattice spacings, with a second fiber population in the core of the bundle shrunken by ~15%, a fairly common finding with tannic acid fixation.
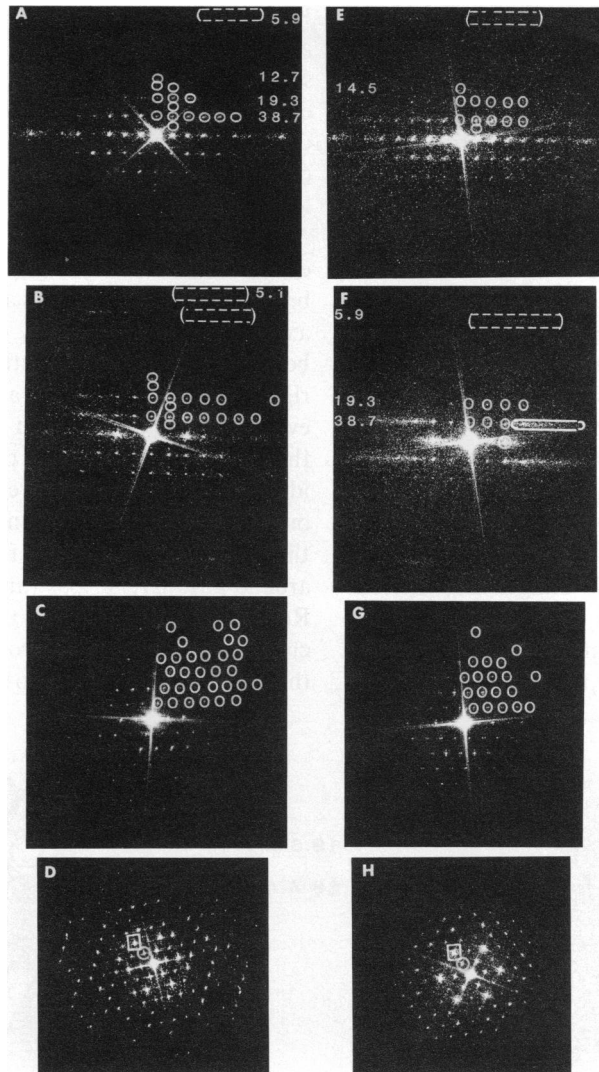
FIGURE 7 Optical transforms of rigor (*left*) and S1-loaded (*right*) myac and actin layers and 100-nm and 15-nm cross sections are shown. Circled spots (○) in *A–C* and *E–G* represent (in one quadrant) those included in optical filtering masks: (*A*) rigor myac layer; (*B*) rigor actin layer; (*C*) 15-nm cross section of rigor; (*D*) 100-nm rigor cross section; (*E*) S1 myac layer; (*F*) S1 actin layer; (*G*) 15-nm cross section of S1; (*H*) S1-loaded 100-nm cross section. In *D*, *H*, 10.0 spots are marked by a circle (○), 20.0 spots by a square (□). Note preservation of the 5.1 and 5.9 nm actin layer lines. Also, in cross sections, the 20.0/10.0 ratios are comparable to rigor and S1 x-ray equatorial ratios, respectively (Fig. 2).

Mechanical Measurements on S1-labeled Fibers

Any displacement of rigor cross-bridges upon S1 incubation should also be detected by a change in the mechanical properties of muscle fibers. Experiments of this type were done both on bundles of ~3–5 fibers and on single fibers, with qualitatively similar results in both cases. Measurements using an interference microscope to monitor changes of optical path length across a single fiber, as described by Endo and Iino (1980), indicated that at S1 concentrations of 6–7 mg/ml, between 10 and 20 min were needed for saturation (~16% IOPD increase) at room temperature, and measurements of tension and stiffness of both single

fibers and of fiber bundles showed no detectable change in tension or stiffness after this period of time or even up to 1 h. This indicates that significant cross-bridge displacement did not occur, in agreement with the electron microscopic evidence described above.

Reversibility of S1 Binding

As an ideal, our experiments involve reversible binding of the S1 ligand to rigor muscle, even though none of the quantitative data are derived from or dependent on the reversibility of the S1 binding. In practice, perfect reversibility has yet to be consistently attained. This problem was explored in several lines of experiment.

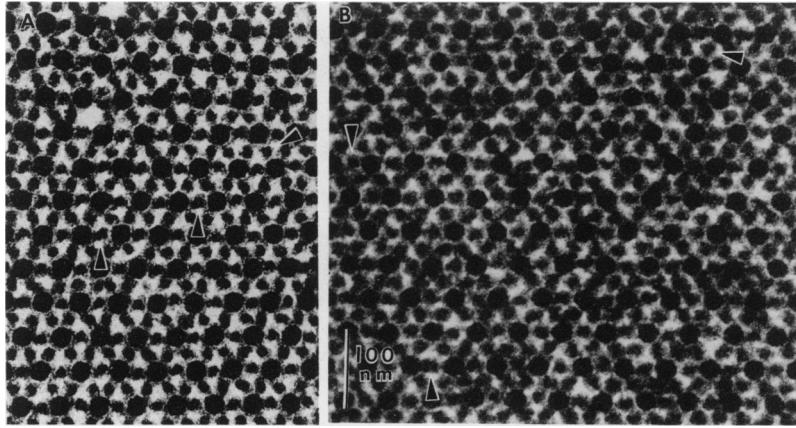In mechanical experiments described above, immersion

FIGURE 8   100-nm cross sections of (*A*) rigor and (*B*) S1-loaded fibers are shown. The filaments are uniformly surrounded by a haze of density in S1-loaded fibers that is missing in the rigor fibers. The hazy added material appears to stain less intensely than the original cross-bridges, a distinction more obvious in these thick sections than in thinner (20 nm) sections. Arrowheads mark paired densities indicating rigor cross-bridge labeling (see text). Such transverse views showed full decoration penetrating throughout the fibrils. This supplements evidence for uniform decoration along the filament axis gained from longitudinal sections.
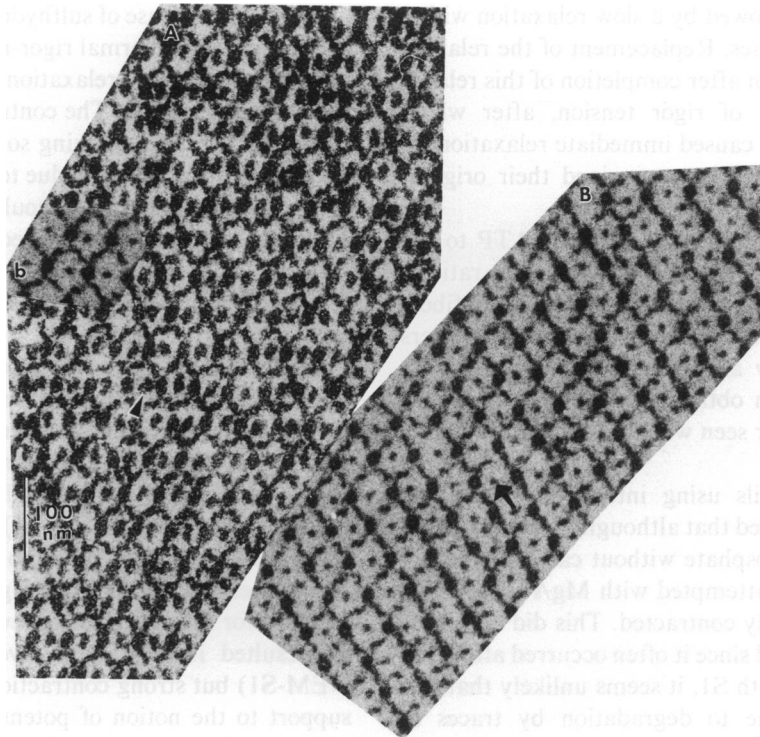

FIGURE 9   15-nm cross sections of (*A*) S1-loaded and (*B* and *b* inset) rigor at identical magnifications (but showing different directions and amounts of section compression) are shown. The two thin filaments (out of the six around each thick filament) that do not in rigor receive bridges at this level (nonbridged actins; arrows in *B*) are dramatically enlarged by S1 binding (black on white triangle in *A*). These S1 decorated features show characteristic oblong profiles of consistent orientation, rather than the circular hazy density seen in Fig. 8, due to the short segment of actin helix included within a 15-nm section. Rigor cross-bridges that form the flared X are also clearly present after S1 loading, and are slightly increased in density and size. This is consistent with the notion that while rigor cross-bridges may include two endoheads, the depth of a 15-nm section includes three actin monomers per long-pitch strand, and any remaining free in rigor can be occupied by exoheads.
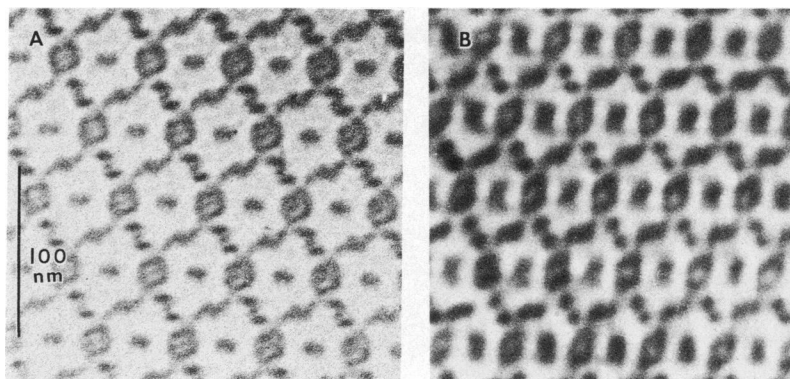
FIGURE 10   Filtered images of 15-nm cross sections of (A) rigor and (B) S1-loaded fibers at identical magnifications (but with unequal section-compression distortions). The limbs of the flared X as well as the nonbridged actins are increased in density in the S1-loaded fibrils, but the flared X arms are not simply rotation isomers of the loaded form of nonbridged actins; they include distinguishing features (stems joined to thick filaments, and differences between left and right limbs of each X in density distribution and outline; Reedy and Reedy, 1985), which indicate persistence of rigor-bridging by endoheads. In rigor, actin twofold orientation at the nonbridged level of thin filaments is averaged as an oblong or two-dot profile. Taking the actin azimuth from this, we can deduce the correctness of Taylor and Amos (1981) binding geometry from the hand, slew, and curvature of the density added when S1 binds to the nonbridged actins (see Fig. 13).

of fibers in a standard relaxing solution following incubation in S1 did not lead to the usual rapid relaxation (<1 s) seen with rigor fibers, which occurs at a rate apparently limited only by the diffusion of ATP. Instead, a transient contraction was seen, followed by a slow relaxation with a half-time of several minutes. Replacement of the relaxing solution by a rigor solution after completion of this relaxation led to development of rigor tension, after which renewed addition of ATP caused immediate relaxation, so that the fibers appeared to have regained their original properties.

In x-ray experiments, addition of 5 mM ATP to the S1-labeled fibers resulted in a rapid change in the ratio of the equatorial peaks to that characteristic of relaxed fibers (20.0/10.0 = ~0.6). However, the structure of the fibers deteriorated considerably as judged by the increasingly diffuse scattering pattern obtained over the next several hours. This effect is never seen when fresh rigor fibers are exposed to ATP.

Experiments on fibrils using interference or phase contrast microscopy showed that although bound S-1 could be removed with pyrophosphate without causing contraction, when removal was attempted with MgATP relaxing solution, the fibrils usually contracted. This did not occur with unlabeled fibrils, and since it often occurred after very short incubation times with S1, it seems unlikely that this effect was primarily due to degradation by traces of proteolytic enzymes in the S1 preparations.

A possible explanation of the contraction and resultant deterioration of the muscles when ATP is added to reverse exo-S1 binding is that a certain fraction of the exo-S1 bound to the fibers dissociates very slowly, even in the presence of ATP, and that these S1 molecules lead to an activation of the thin filament regulatory system (potentiation; Bremel and Weber, 1972) even when EGTA is present without added calcium. It is known that extensive

modification of the SH groups of S1 can give species that bind strongly to thin filaments even in the presence of ATP (Pemrick and Weber, 1976), and it seems likely that the S1 preparations used contained a fraction with these properties, possibly because of sulfhydryl oxidation. The observed restoration of the normal rigor-relaxation properties of the fibers once complete relaxation had been achieved agrees with this explanation. The contraction of S1-loaded fibrils in Mg-ATP-EGTA relaxing solution as observed by light microscopy is presumably due to the same cause (although in this case reversibility could not be demonstrated). Likewise, contraction activated by unreleased S1 could explain the loss of structure observed on addition of relaxing solution to large fiber bundles after prolonged exposure to S1.

In agreement with this interpretation, we have now shown in preliminary experiments that the principal result reported above, i.e., the transient contraction after adding relaxing solution to S1-labeled rigor fibers, could be reproduced even more dramatically using SH-modified S1 N-ethyl maleimide (NEM-S1) and using much shorter incubation times. In addition to this, inclusion of NEM-S1 in an otherwise normal relaxing solution as an incubation medium for fibers that had previously not been exposed to S1 resulted in a gradual (over ~10 min at 6 mg/ml NEM-S1) but strong contraction. This result lends strong support to the notion of potentiation by modified, ATP-resistant S1, and incidentally confirms the phenomenon of potentiation for insect flight muscle.

DISCUSSION OF NUMBER OF BOUND MYOSIN HEADS AND NUMBER OF AVAILABLE MYOSIN-BINDING SITES IN RIGOR

The results described above favor certain interpretations concerning the most likely number of myosin molecules per
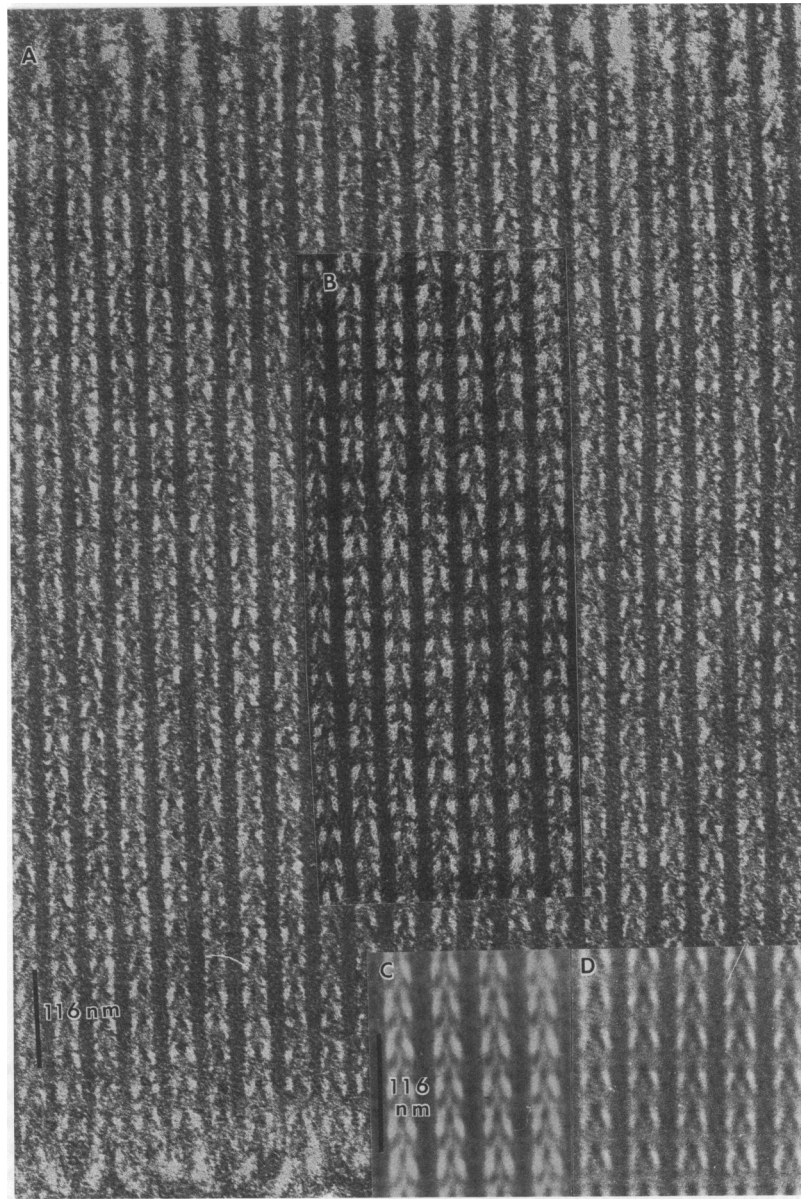
162

FIGURE 11 (*A*) S1-loaded and (*B*) rigor myac layer at the same magnification, and (*C*) rigor and (*D*) S1 filtered images at 10% higher magnification are shown. The differences are not dramatic, for the simple reason that the axial tilt and azimuthal slew of chevrons from endohead binding fit well into the arrowhead profiles produced by full decoration with exo S1. The double chevrons appear more filled in after S1-loading, but bridge connections to the thick filament are still evident.

crown (per 14.5 nm of each thick filament) of insect flight muscle, and the number of these heads that are attached to actin per crown cell in the rigor state. Taking the results from gel electrophoresis and interference microscopy together, the best numerical agreement between these two methods would be obtained using a model in which there are five myosin molecules (ten heads) per crown cell.[1] However, this agreement is considered to be fortuitous. It is

probably a result of the combined errors of the two approaches, e.g., the value from gel electrophoresis may be underestimated by up to 10%. Also, the twofold rotational symmetry of thick filaments of rigor muscle is not compatible with fivefold symmetry of isolated thick filaments.

For these reasons, our discussion will be confined to the two prevailing models with four or six myosins per crown. The relationships of these two models to the results obtained here are presented in Table I. We would like to reemphasize several points that are necessary to evaluate the information contained in Table I. First, the intensity of the outer actin layer lines in the x-ray diffraction patterns is expected to increase after S1 loading with the square of

---

[1]The measured ratio of S1 heads to myosin heads of 0.92 would lead to a value of 9.2 for the number of S1 heads that can bind to the rigor lattice, in good agreement with the value of 9.11 obtained from interference microscopy, which is independent of the number of myosins per crown.
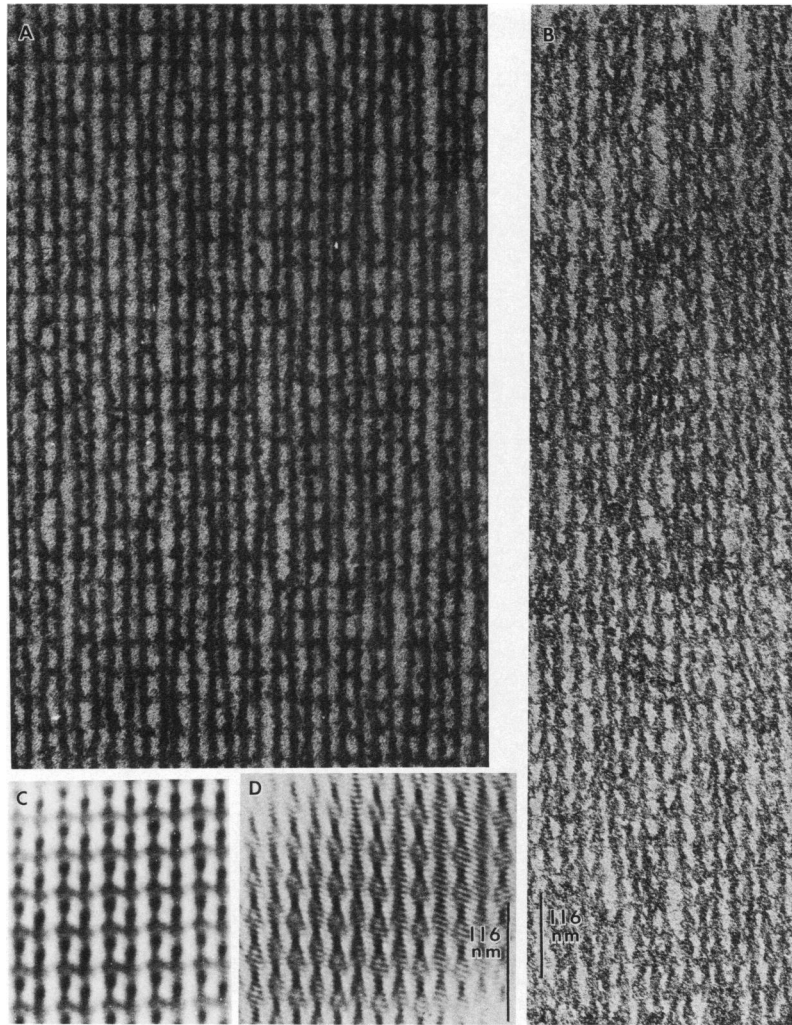
FIGURE 12 (A) Actin layers from rigor and (B) S1-loaded fibers at the same magnification, with their filtered images, (C) rigor and (D) S1 at 35% higher magnification are shown. The rigor and S1-loaded actin layers differ much more obviously than do myac layers. This S1 actin layer is from the same sarcomere and section as the myac layer in Fig. 11, so the two views are optimally comparable. In this view, the connections of the endogenous heads to the thick filaments have been sectioned away, and a distinction between endogenous heads and exogenous S1 is no longer readily apparent. The markings on adjacent thin filaments maintain a 12.9 nm (38.7/3 nm) stagger (C), but S1 markedly obscures the beads and rungs features (D) that typify rigor expression of rear vs. lead chevrons in their actin layer presentation (see Reedy and Reedy, 1985).

the amount of electron density that scatters according to the actin filament symmetry. Therefore, the measured increase of four to fivefold indicates that incubation in S1 approximately doubles the occupancy of the actin sites, implying a 1:1 ratio for exogenous S1 heads to endogenous heads bound as cross-bridges. Second, actin occupancy by bound endogenous heads cannot be much below half of the 15.75 actin sites per crown cell, otherwise the increase from S1 binding to vacant sites would exceed the 1:1 exo/endoheads ratio indicated by layer-line changes. At the same time, actin occupancy by endogenous heads cannot be much over half of 15.75, or there would be too few actin sites left to bind the nearly equal number of exogenous S1 heads required by x-ray and gel ratios or to bind the 9.11 exoheads indicated by interference microscopy.

Concerning the number of myosin heads per crown,

Table I reveals that regardless of the number of endoheads bound in rigor, six myosins/crown appears too many, since the gel-derived ratio of 0.92 would then require 11.04 exogenous S1 heads to bind; this exceeds the value of 9.1 obtained from interference microscopy (which is independent of the number of thick filament heads) and would force us to conclude from the layer-line intensity increase that 11 endogenous heads were already bound. 11 (or even 9) exo-S1 heads added to 11 endoheads would require more than the 15.75 actin sites available per crown cell. Models with four myosins per crown do not encounter these difficulties and are thus favored by our evidence.

The number of endogenous myosin heads attached as cross-bridges in insect flight muscle may be significantly less than the total number available (Lovell et al., 1981; Offer and Elliot, 1978; Holmes et al., 1980). In contrast, in
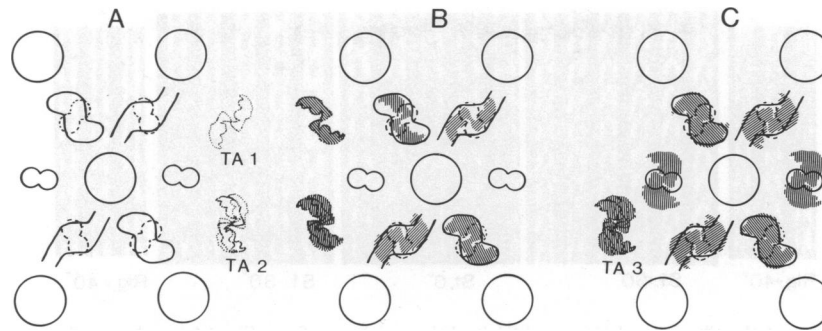
FIGURE 13   A tracing of averaged flared X structure overlaid with projections (scaled to the same magnification) of one, two, or three levels of acto-S1 complex according to the geometry of Taylor and Amos (1981) are shown. (*A*) Outline of flared X from Reedy and Reedy (1985). Averaged nonbridged thin filaments show actin twofold orientation in the gap between double chevrons. The azimuth of actin twofold (dashed outline) is not seen in limbs of flared X, but is inferred from 60° rotation required by actin lattice (Reedy, 1968). Dotted outlines indicate one level (*TA1*) and two levels (*TA2*), the latter rotated to follow the 26° per monomer twist of the actin helix. In *B*, these dotted outlines have been replaced by striped shading. When Taylor-Amos profiles are superimposed on flared X limbs, guided by the inferred actin azimuth, then the S1 features of Taylor-Amos model fit very well to cross-bridges. It is clear that two heads bound with Taylor-Amos geometry give a better fit to cross-bridges than one head. In *C* (S1-loaded), *TA3* is a projection of three levels of the acto-S1 complex. This is the maximum number of complexes that can be included in 15 nm cross sections. Adding S1 heads with Taylor-Amos geometry to all available actins produces the shapes seen here, thickening flared X limbs somewhat, and dramatically expanding the profile at the nonbridged actins (as shown in Fig. 10 *B*). The density added by S1 binding to the known actin azimuth at this level reproduces the shape and orientation of head plus actin geometry from Taylor and Amos. This constitutes independent evidence for the Taylor-Amos geometry of S1 attachment to actin.

vertebrate muscle 95–100% of heads appear to be attached (Lovell et al., 1981; Thomas and Cooke, 1980). In a recent publication using the spin-label EPR technique, Thomas et al. (1983) have attempted to measure the number of attached heads in rigor flight muscle from dung beetles, and while finding no evidence for a large number of detached bridges (e.g., 50%), they could not decide definitely between 80 and 100% heads bound. The specific geometrical arrangement of myosin heads and actin targets in *Lethocerus* flight muscle may not permit attach-

ment of all myosin heads even in the presence of an excess of actin monomers (Squire, 1972; Reedy and Garrett, 1977; Wray, 1979b). Such a lattice arrangement may also be responsible for stretch activation (Wray, 1979b), and for the distinctive structural response to APPNP detected by x-rays (Wray, J. S., manuscript in preparation).

The important model of Offer and Elliott (1978) proposes that only four myosin heads per crown are bound as cross-bridges in *Lethocerus* muscle in rigor. The flared X seen at each cross-bridge level in 15 nm cross sections of
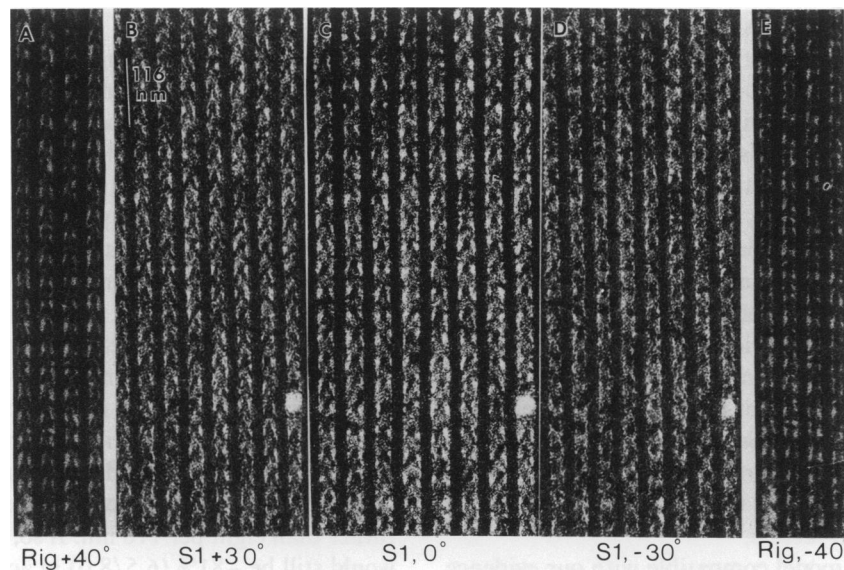

FIGURE 14   Tilt views of myac layers from rigor *A*, +40° and *E*, −40°) and S1-loaded (*B*, +30°, *C*, untilted, and *D*, −30°) fibers are shown. The tilt axis is along the long axis of the fiber. Rigor cross-bridge structure is still evident in S1 loaded fibers; see also averaged images in Fig. 15.
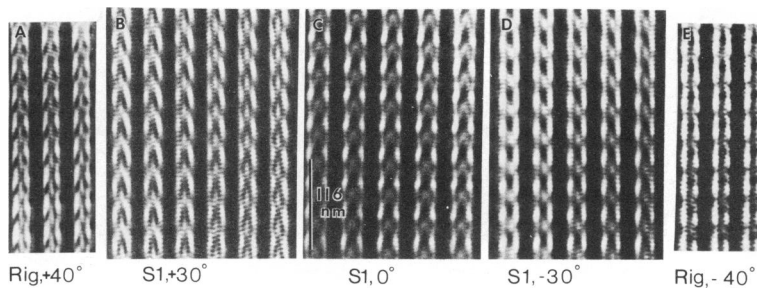
Rig,+40°   S1,+30°   S1, 0°   S1, -30°   Rig,- 40°

FIGURE 15   Filtered images of the tilt views of rigor and S1-loaded myac layers from Fig. 14 are shown. The averaged image patterns resulting from double chevrons remain evident in the S1-loaded fibers (*C*, untilted view), indicating that exogenous S1 has not replaced rigor cross-bridges on a regular basis. In both *A* (rigor) and *B* (S1) the double bead pattern straddling actin and arising from the lead chevron can be seen, whereas in both *D* (S1) and *E* (rigor) the single dense bead centered on actin at the level of the rear chevron is apparent. The fact that these appearances in S1-loaded myac layers still vary with tilt, rather than simply translating axially, indicates a rigorlike structure at the levels of lead and rear chevrons that differs in uniformity and order from that found along the segments of actin that have become occupied by S1. Some of this difference may be due to poorer preservation of the untethered S1, but some of it probably remains faithful to original differences between exo-S1 and the endoheads forming rigor bridges.

rigor indicates an obvious minimum of four heads bound per crown. Table I shows that four myosin endoheads bound per crown would leave 11.8 sites free to bind endogenous S1 heads. However, adding more than four exo-S1 heads to fill vacant actin sites would increase layer-line intensity more than the four to fivefold observed, whereas filling fewer than eight sites would force us to infer from the gel ratio that thick filaments contain only two or three myosins per crown, which does not agree with any available evidence. Adding fewer than 11.8 exoheads per crown cell should also produce obvious gaps in the electron micrographs of S1-loaded muscle, and we find none. If endo- and exo-S1 heads together occupied only 8 out of 15.8 actin monomers, this still leaves 7.8 blocked by additional factors. These reasons prompt us to consider what factors other than cross-bridges could prevent exogenous S1 from binding to unbridged actin monomers in rigor. There is no reason to suppose that penetration is restricted, because the deepest filaments seem as heavily decorated as those outermost in fibrils and fibers. One possibility is that the 2.2 troponin complexes per crown cell might block one or two heads. Although studies on the binding of S1 to regulated actin in solution indicate that the stoichiometry of binding is not influenced by the presence or absence of troponin, and is accurately 1:1 (S1/actin monomer) (Greene and Eisenberg, 1980), these studies were with proteins from rabbit muscle. Troponin from insect flight muscle is twice as large as its vertebrate counterpart (Bullard, 1984) and it is conceivable that this could block S1 binding to one or two monomers. Nevertheless, the PAGE ratio and the interference microscopy presented here are difficult to reconcile with blocking of as many as 7.8 actin monomers, whether by troponin, steric hindrance, or unknown factors.

The most probable model compatible with our evidence appears to be one with eight heads per crown, of which six to seven are bound to thin filaments in rigor. Using the

higher numbers from our data, if we add seven endogenous heads to the nine exoheads indicated by interference microscopy, the total occupany per crown cell exceeds only slightly the maximum of 15.75 actin monomers. If we take the lower number compatible with our data, six heads bound, together with 7.4 additional exoheads from gel data, this leaves 2.4 actin monomers blocked by additional factors.

It seems likely that on average a nonintegral number of endogenous heads, between six and seven, are bound per crown cell to thin filaments in the rigor state of insect flight muscle. Our average value need not suggest that every group of four bridges averages 6.5 heads. The flared × cannot be identical at all levels, but should vary over successive repeats of 14.5 nm in each 116 nm long period (Reedy and Garrett, 1977). Some flared ×s may commit all eight heads to the four cross-bridges. The rest are probably less ideally and fully populated, owing to awkward geometry in matching eight crowns of myosin origins to an actin lattice with nine levels of actin target zones in every 116 nm. The excess of target zones might be expected to facilitate full binding of all endoheads, but since our results and tryptic digestion (Lovell et al., 1981) suggest that binding is only 70–80% complete, we presume the target zone excess must be offset by missed contacts in the region of worst vernier mismatch between origins and target zones.

A last point of numerical correspondence deserves note. The crown of eight myosin heads is described for the 14.5 nm myosin repeat, as seen in relaxed muscle and in isolated thick filaments (Reedy et al., 1981). In rigor, this period is obscured, and the flared × structural repeat of four cross-bridges may well occur at nine levels (every 12.9 nm) rather than eight per 116 nm. If so, then endohead binding would still be ~81% (6.5/8.0) in accord with our findings. In a 12.9 nm target cell, only 14.0 actin subunits and 7.1 myosin heads are available. The average composition of

flared $\times$s would be 5.8 heads. This value is very close to the six heads per 12.9 repeat, which can be inferred from the three-dimensional reconstruction of rigor cross-bridges in *Lethocerus* flight muscle (Taylor et al., 1984). In this work, lead and rear cross-bridges in the double chevron were shown to have similiar volumes but different average densities, suggesting that lead chevrons may average two

FIGURE 16 (*A*) A single +45° view of S1-loaded and (*B*) rigor myac layers tilted round an axis tranverse to the long axis of the fiber are shown. On the *left* side of the thick filaments and *right* side of thin filaments, the bridges make a strong, single bar connecting to the thin filament, whereas on the opposite side (*right* side of thick and *left* side of thin filaments) the bridges appear double or diffuse. This suggests that the helical arrangement of attached rigor cross-bridges is still intact (Reedy and Reedy, 1985).

heads per bridge, whereas rear chevrons average one head. Since the part of each flared $\times$ assignable to a single thick filament comprises two lead bridges and two rear bridges, this interpretation gives an average of six heads per flared $\times$.

CONCLUSIONS

The results reported here confirm that the lattice of thick and thin filaments in glycerinated insect flight muscle can be penetrated by S1, and that under rigor conditions a large number of binding sites on thin filaments are available to exogenous S1. Under the conditions used, cross-bridge displacement by S1 appears to be negligible. The gel-indicated ratio of bound exogenous S1 to total endogenous myosin gives a much better fit to thick filament models with four myosins per crown (Wray, 1979a, b; Reedy et al., 1981; Aust et al., 1980) than to those with six.

The interpretation of the S1 binding experiments in terms of the exact number of myosin heads that are attached to thin filaments in rigor is hampered by lack of information concerning the possible blocking of binding sites by troponin. However, the most reasonable interpretation of the quantitative binding data, as selected using the increase in intensity of the x-ray diffraction pattern, indicate that 6 to 7 (75–85%) of the 8 endogenous heads are bound to the thin filaments in rigor. The degree of final occupancy of thin filaments after saturation with S1 appears to be at least 85%. Thus it is justified to treat the x-ray scattering on the actin-based layer lines of S1-saturated muscle as arising from an array of fully decorated thin filaments. This presumption has already played a critical role in three publications. In the first, x-ray data from S1-saturated muscle provided part of the basis for x-ray modeling of rigor cross-bridge shape (Holmes et al., 1980), because bound S1 is believed identical to the cross-bridge portion that scatters with actin symmetry. In another, these x-ray data were combined with phase data from Fourier analysis of EM images of decorated actin to refine a computer model of decorated actin (Holmes et al., 1982). In the third, the x-ray layer line intensities from S-1 loaded fibers guided selection of decorated actin images for three-dimensional reconstruction of the best-preserved structure (Amos et al., 1982).

Comparison of 15-nm cross-sectional images of rigor and S1 loaded muscle suggests that exogenous myosin heads bind to actin with Taylor-Amos binding geometry (Taylor and Amos, 1981), and in fact gives independent evidence supporting this model of the binding geometry, adding to the supporting evidence inferred (Reedy and Reedy, 1985) and observed (Taylor et al., 1984) in connection with endogenous bound heads. However, cross-bridges differ in shape from bound S1, especially more distal to the thin filament; this is presumably because the endoheads are tethered to thick filaments, whereas exoheads are not.
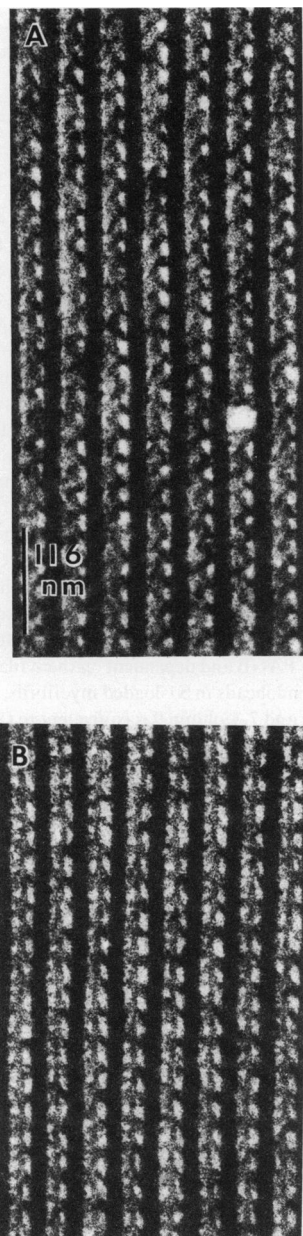
TABLE I
S1 BINDING MEASUREMENTS VS. RIGOR MODELS

Models		Quantitative interference microscopy				Quantitative PAGE gels			
Total endoheads	Endoheads bound	S1 exoheads bound	Total bound heads	Actin sites vacant	X-ray intensity increase expected (vs. 4–5 measured)	S1 exoheads bound	Total bound heads	Actin sites vacant	X-ray intensity increase expected (vs. 4–5 measured)
(per crown)		(per crown cell)				(per crown cell)			
assumed 1	assumed 2	measure 3	calculated 4	calculated 5*	calculated 6	measured 7	calculated 8	calculated 9*	calculated 10
12	4	9.11	13.11	2.64	10.7	11.04	15.04	0.7	14.1
12	5	9.11	14.11	1.64	8.0	11.04	16.04	−0.3	10.3
12	6	9.11	15.11	0.64	6.3	11.04	17.04	−1.3	8.1
8	4	9.11	13.11	2.64	10.7	7.36	11.36	4.4	8.1
8	5	9.11	14.11	1.64	8.0	7.36	12.36	3.4	6.1
8	6	9.11	15.11	0.64	6.3	7.36	13.36	2.4	5.0
8	7	9.11	16.11	−0.36	5.3	7.36	14.36	1.4	4.2
8	8	9.11	17.11	−1.36	4.6	7.36	15.36	0.4	3.7

The table shows how the several measurements obtained here constrain the choice of models, both for thick filaments and for the number of endoheads bound as cross-bridges in rigor. The choices that best agree with all measured parameters indicate a model with four myosins and thus eight heads/crown, with ~80% (between six and seven endoheads per crown cell) attached to actin in rigor. Column 1 indicates the total number of endogenous heads available per crown (i.e., per 14.5-nm repeat) for two prevailing models of insect flight muscle thick filaments, with either six or four myosins per crown. Column 2 proposes various numbers of endogenous heads attached to thin filaments in rigor. Column 3 indicates S1 (exogenous) heads bound per crown cell by interference microscopy of fibrils. (A crown cell is 14.5 nm long, 58 nm on a side, and contains 1 crown of endoheads and 15.75 actin monomers.) Sarcomere dry mass increase of 20.13% due to S1 is independent of models in columns 1 and 2. Exohead number is calculated from S1 MW of 115 kd, baseline dry mass of 4,320 kd per crown cell, and 83% as fraction of sarcomere mass which contains crown cells to which S1 can bind. Column 4 is the sum of columns 2 and 3. Column 5 indicates that the value (15.75 actin sites per crown cell) − (value in column 4) is equal to the number of actin sites per crown cell still lacking bound heads if S1 loading produces the total actin occupancy given in column 4. Negative values indicate excess of bound heads over available actin sites. Column 6 shows the intensity ratio, or the factor by which actin layer line intensity should increase after loading with S1 exo-heads, = [(column 4)/(column 2)]². Column 7 is equivalent to column 3, except determined by PAGE and dependent on thick filament model, which is equal to 0.92 × (column 1). 0.92 is the molar heavy-chain ratio of (rabbit) exoheads to (insect) endoheads in S1-loaded myofibrils, after correction for the staining difference between (rabbit) S1 and (rabbit) myosin. Column 8 is the sum of columns 2 and 7. Column 9 is equivalent to (15.75 actin sites per crown cell) − (value in column 8). The values in column 10 were obtained by squaring the (column 8)/(column 2) ratio.

*If actin sites are blocked one-to-one by troponin as effectively as by rigor cross-bridges, then 2.25 (troponins per crown cell) should be subtracted from all values in columns 5 and 9. Thick filaments with six myosins per crown would now conflict even more with x-ray and PAGE measurements. Thick filaments with four myosins/crown could have four to five endoheads bound (interference microscopy), but this should lead to twice the observed four to fivefold increase in x-ray intensity; if the same thick filament model has six to seven heads bound, agreement is reasonable for PAGE gels and x-rays, but the interference microscope count of exoheads bound would now exceed by about two sites the capacity of each crown cell.

REFERENCES

Amos, L. A., H. E. Huxley, K. C. Holmes, R. S. Goody, and K. A. Taylor. 1982. Structural evidence that myosin heads may interact with two sites on F-actin. *Nature (Lond.).* 299:467–469.

Aust, S., P. Hinkel, and G. Beinbrech. 1980. Evidence for four-stranded myosin filaments in honey bee flight muscle. *J. Muscle Res. Cell Motil.* 1:448.

Barrington Leigh, J., and G. Rosenbaum. 1976. Synchrotron x-ray sources: a new tool in biological structural and kinetic analysis. *Annu. Rev. Biophys. Bioeng.* 5:239–270.

Bremel, R. D., and A. Weber. 1972. Cooperation within actin filament in vertebrate skeletal muscle. *Nature (Lond.).* 238:97–101.

Bullard, B. 1984. A large troponin in asynchronous insect flight muscle. *J. Muscle Res. Cell. Motil.* 5:196.

Bullard, B., and M. K. Reedy. 1973. How many myosins per crossbridge? II. Flight muscle myosin from the blowfly, *Sarcophaga bullata. Cold Spring Harbor Symp. Quant. Biol.* 37:423–428.

Chaplain, R. A., and R. T. Tregear. 1966. The mass of myosin per cross-bridge in insect flight muscle. *J. Mol. Biol.* 21:275–280.

Endo, M., and M. Iino. 1980. Specific perforation of muscle cell membranes with preserved SR functions by saponin treatment. *J. Muscle Res. Cell. Motil.* 1:89–100.

Goldstein, D. J., and I. J. Hartmann-Goldstein. 1974. Accuracy and precision of a scanning and integrating microinterferometer. *J. Micros. (Oxf.).* 102:143–164.

Greene, L. E., and E. Eisenberg. 1980. Cooperative binding of myosin subfragment-1 to the actin-troponin-tropomyosin complex. *Proc. Natl. Acad. Sci. USA.* 77:2616–2620.

Holmes, K. C., R. S. Goody, and L. A. Amos. 1982. The structure of

S1-decorated actin filaments calculated from x-ray diffraction data with phases derived from electron micrographs. *Ultramicroscopy.* 9:37–44.

Holmes, K. C., R. T. Tregear, and J. Barrington Leigh. 1980. Interpretation of the low angle x-ray diffraction from insect muscle in rigor. *Proc. R. Soc. Lond. B. Biol. Sci.* 207:13–33.

Konrad, M., and R. S. Goody. 1982. Kinetic and thermodynamic properties of the ternary complex between F-actin, myosin subfragment 1 and adenosine 5'-[beta, gamma-imido]triphosphate. *Eur. J. Biochem.* 128:547–555.

Lovell, S. J., P. J. Knight, and W. F. Harrington. 1981. Fraction of myosin heads bound to thin filaments in rigor fibrils from insect flight and vertebrate muscles. *Nature (Lond.).* 293:664–666.

Lowey, S., H. S. Slayter, A. G. Weeds, and H. Baker. 1968. Substructure of the myosin molecule. I. Subfragments of myosin by enzymic degradation. *J. Mol. Biol.* 42:1–29.

Offer, G., and A. Elliott. 1978. Can a myosin molecule bind to two actin filaments? *Nature (Lond.).* 271:325–329.

Pemrick, S., and A. Weber. 1976. Mechanism of inhibition of relaxation by N-ethylmaleimide treatment of myosin. *Biochemistry.* 15:5193–5198.

Potter, J. D. 1974. The content of troponin, tropomyosin, actin and myosin in rabbit skeletal muscle myofibrils. *Arch. Biochem. Biophys.* 162:436–441.

Reedy, M. K. 1968. Ultrastructure of insect flight muscle. I. Screw sense and structural grouping in the rigor cross-bridge lattice. *J. Mol. Biol.* 31:155–176.

Reedy, M. K., and W. E. Garrett. 1977. Electron microscope studies of *Lethocerus* flight muscle in rigor. *In* Insect Flight Muscle: Proceedings of the Oxford Symposium. R. T. Tregear, editor. Elsevier, Amsterdam. 115–136.

Reedy, M. K., and C. Lucaveche. 1984. A-band mass exceeds mass of its filament components by 30–45%. *In* Contractile Mechanism in Muscle. G. H. Pollack and H. Sugi, editors. Plenum Publishing Corp., New York. 29–46.

Reedy, M. K., and M. C. Reedy. 1985. Rigor cross-bridge structure from flared X and tilt views of single filament layers in insect flight muscle. *J. Mol. Biol.* In press.

Reedy, M. K., G. F. Bahr, and D. A. Fischman. 1973. How many myosins per cross-bridge? I. Flight muscle myofibrils from the blowfly, *Sarcophage bullata. Cold Spring Harbor Symp. Quant. Biol.* 37:397–421.

Reedy, M. K., K. R. Leonard, R. Freeman, and T. Arad. 1981. Thick filament mass determination by electron scattering measurements with the scanning transmission electron microscope. *J. Muscle Res. Cell Motil.* 2:45–64.

Reedy, M. K., R. S. Goody, W. Hofmann, and G. Rosenbaum. 1983. Coordinated EM and x-ray studies of glycerinated insect flight muscle. I. X-ray diffraction monitoring during preparation for electron microscopy of muscle fibers fixed in rigor, in ATP and in AMPPNP. *J. Muscle Res. Cell Motil.* 4:25–53.

Rosenbaum, G. 1979. The use of synchrotron radiation for x-ray structure analysis in molecular biology. Ph.D. thesis, University of Heidelberg, Heidelberg, Federal Republic of Germany. 180.

Squire, J. M. 1972. General model of myosin filament structure. II. Myosin filaments and cross-bridge interactions in vertebrate striated and insect flight muscles. *J. Mol. Biol.* 72:125–138.

Taylor, K. A., and L. A. Amos. 1981. A new model for the geometry of the binding of myosin cross-bridges to muscle thin filaments. *J. Mol. Biol.* 147:297–324.

Taylor, K. A., M. C. Reedy, L. Cordova, and M. K. Reedy. 1984. Three-dimensional reconstruction of rigor insect flight muscle from tilted thin sections. *Nature (Lond.).* 310:285–291.

Thomas, D. D., and R. Cooke. 1980. Orientation of spin-labeled myosin heads in glycerinated muscle fibers. *Biophys. J.* 32:891–906.

Thomas, D. D., R. Cooke, and V. A. Barnett. 1983. Orientation and rotational mobility of spin-labeled myosin heads in insect flight muscle in rigor. *J. Muscle Res. Cell Motil.* 4:367–378.

Tregear, R. T., and J. Squire. 1973. Myosin content and filament structure in smooth and striated muscle. *J. Mol. Biol.* 77:279–290.

Weeds, A., and R. S. Taylor. 1975. Separation of subfragment 1 isoenzymes from rabbit skeletal muscle myosin. *Nature (Lond.).* 257:54–56.

White, D. C. S. 1970. Rigor contraction and the effect of various phosphate compounds on glycerinated insect flight and vertebrate muscle. *J. Physiol. (Lond.).* 208:583–605.

Wray, J. S. 1979*a*. Structure of the backbone in myosin filaments of muscle. *Nature (Lond.).* 277:37–40.

Wray, J. S. 1979*b*. Filament geometry and the activation of insect flight muscles. *Nature (Lond.).* 280:325–326.

Wray, J. S. 1984. Cross-bridge states in invertebrate muscles. *In* Contractile Mechanisms in Muscle. G. H. Pollack and H. Sugi, editors. Plenum Publishing Corp., New York. 185–192.

Ziegler, A., S. Harrison, and R. Leberman. 1974. The minor proteins in tomato bushy stunt virus. *Virology.* 59:509–515.